

EvHandPose: Event-based 3D Hand Pose Estimation with Sparse Supervision

Jianping Jiang[†], Jiahe Li[†], Baowen Zhang,
Xiaoming Deng[‡], *Member, IEEE*, Boxin Shi[‡], *Senior Member, IEEE*

Abstract—Event camera shows great potential in 3D hand pose estimation, especially addressing the challenges of fast motion and high dynamic range in a low-power way. However, due to the asynchronous differential imaging mechanism, it is challenging to design event representation to encode hand motion information especially when the hands are not moving (causing motion ambiguity), and it is infeasible to fully annotate the temporally dense event stream. In this paper, we propose *EvHandPose* with novel hand flow representations in Event-to-Pose module for accurate hand pose estimation and alleviating the motion ambiguity issue. To solve the problem under sparse annotation, we design contrast maximization and edge constraints in Pose-to-IWE (Image with Warped Events) module and formulate *EvHandPose* in a self-supervision framework. We further build *EvRealHands*, the first large-scale real-world event-based hand pose dataset on several challenging scenes to bridge the domain gap due to relying on synthetic data and facilitate future research. Experiments on *EvRealHands* demonstrate that *EvHandPose* outperforms previous event-based method under all evaluation scenes with 15 ~ 20 mm lower MPJPE and achieves accurate and stable hand pose estimation in fast motion and strong light scenes compared with RGB-based methods. Furthermore, *EvHandPose* demonstrates 3D hand pose estimation at 120 fps or higher.

Index Terms—3D hand pose estimation, event camera.

1 INTRODUCTION

HAND pose estimation plays a key role in computer vision, human-computer interaction, virtual reality, and robotics [1]. Most of the existing vision-based hand pose estimation approaches adopt conventional imaging sensors such as RGB or RGB-D cameras. Although these sensors are widely available and effective for various hand pose relevant applications, due to the limitations from their imaging mechanisms, it is still challenging to achieve robust and accurate hand pose results in many real scenarios, especially for those with fast motions and abrupt changes of lighting conditions. Event cameras [2] that generate neuromorphic events by measuring per-pixel intensity changes asynchronously have shown great potential in many vision tasks such as detection [3], tracking [4], 3D reconstruction [5], flow estimation [6], simultaneous localization and mapping [7], [8], due to the advantages of high dynamic range (HDR, 120 dB), low power consumption, and high temporal resolution (up to 1 μ s). Recently, event cameras have also demonstrated their potential in robust 3D hand pose estimation for scenes with fast motions and broad dynamic range, because of their rich temporal information and HDR property [9].

Due to the lack of appearance and texture information in event streams, estimating hand poses using events faces three key challenges as shown in Figure 1 (C1)-(C3). First, from the data inherent properties perspective, asynchronous event streams are spatially sparse and temporally dense, so existing image-based

hand pose estimation solutions can not be directly applied to events. A straightforward solution is to reconstruct intensity frames from events via an “integration” process as [10] and [11]. However, such strategies would sacrifice the advantage of temporally fast and dense events, and it is still an open problem to design effective event representation and feature extractor for event-to-image conversion without losing these advantages. Moreover, event cameras suffer from the motion ambiguity issue, since the static hand parts can not generate events under the assumption of brightness consistency, which may result in that different hand poses generate the same event stream (only relative motion is recorded). Second, it is generally infeasible to annotate the asynchronous event stream using existing hand pose annotation techniques. For annotators, they could only provide sparsely annotated hand poses by sampling the key frames along the temporal dimension of event streams, so the event-based hand pose model is expected to be learned with sparse hand supervision in the temporal dimension. Recently, a pilot study [9] was conducted to learn 3D hand pose from event streams, which uses event simulators to generate synthetic dataset and evaluates the performance on real data. Although promising results are achieved, the third challenge is that the existing method [9] suffers from domain gap between synthetic and real data, since a small real dataset that can not support strong model generalization ability desired for different challenging scenarios.

To address the above challenges, we propose *EvHandPose* – a self-supervision framework to learn event-based 3D hand pose estimation under sparse supervision, as shown in Figure 1 (S1)-(S3). First, in order to deal with the asynchronous data format and motion ambiguity issue, we design specific hand flow representation and apply temporal information to regress the accurate hand pose. And we propose to approximate the hand optical flow in a sequence of event stream by embedding the interpolated hand models. Second, to address the sparse annotation challenge, we apply contrast maximization and edge constraints in a self-supervision framework.

- J. Jiang, B. Shi are with National Engineering Research Center of Visual Technology, School of Computer Science, Peking University, Beijing 100871, China; B. Shi is also with Institute for Artificial Intelligence, Peking University, and Beijing Academy of Artificial Intelligence.
- J. Li, B. Zhang, X. Deng are with Beijing Key Laboratory of Human Computer Interactions, Institute of Software, Chinese Academy of Sciences, Beijing 100190, China, and University of Chinese Academy of Sciences, Beijing, China.
- [†] Equal contribution. [‡] Corresponding authors: shiboxin@pku.edu.cn, xiaoming@iscas.ac.cn

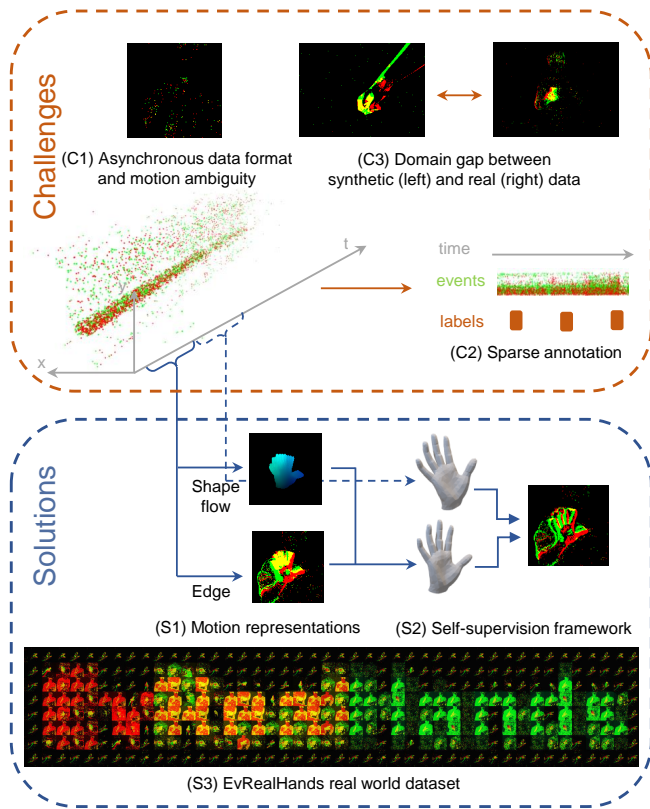


Fig. 1: Hand pose estimation from event data faces several challenges: (C1) asynchronous data format and motion ambiguity issue caused by inherent data properties of events, (C2) sparse annotation with current annotation techniques, (C3) domain gap between synthetic and real data. In order to tackle these issues, we propose *EvHandPose* by extracting novel motion representations including edge and shape flow from event streams with temporal information to predict hand poses (S1). We design a self-supervision framework to tackle the sparse annotation issue (S2). Furthermore, we present the first large real-world event-based hand pose dataset *EvRealHands* (S3) (zoom-in for details).

We first train our Event-to-Pose module on labeled data to get prior knowledge and then fine-tune the model by proposing a self-supervision framework, which is supervised by a Pose-to-IWE (Image with Warped Events) module during training. Finally, to address the domain gap issue limited by synthetic datasets, we construct *EvRealHands*, the first large-scale real event-based hand pose dataset under various challenging scenarios. Experiments demonstrate that our event camera based solution outperforms conventional RGB camera based solutions in challenging scenarios such as fast motion and strong light, and *EvHandPose* achieves hand pose estimation at 120 fps or higher. Our dataset, code and models will be made public after acceptance.

Our main contributions are threefold:

- Novel hand flow representations: Asynchronous event data are effectively processed in Event-to-Pose module for accurate hand pose estimation and alleviating the motion ambiguity issue.
- Self-supervision framework: Pose-to-IWE module is complementarily designed to tackle the sparse annotation issue with contrast maximization and edge constraints specially

designed for the hand.

- Dataset: The first large-scale real dataset *EvRealHands*, consisting of 74 minutes event sequences, 421 K RGB images, with accurate 3D pose and shape annotations is built to tackle the domain gap issue and facilitate future research on event-based hand pose estimation.

2 RELATED WORK

2.1 3D Hand Pose Estimation

Prior arts of 3D hand pose estimation methods consist of appearance-based methods [12], [13], [14], [15], [16] and model-based approaches [17], [18], [19], [20], [21]. Appearance-based methods directly learn the mapping from image space to hand pose space by training on large-scale datasets, which often require large-scale annotated dataset. Model-based methods are designed to fit a prior hand parametric model such as MANO [22] to the image observation. However, these methods require a good initialization for optimization. In order to reduce the expensive annotation cost of large scale dataset, several efforts are adopted to learn hand pose from unlabeled data in weakly-supervised [23], [24], [25], [26] or self-supervised [27], [28], [29] manners. These methods use additional constraints such as segmentation mask, depth, appearance, and biomechanics consistency to ensure the quality of the predicted hand pose. When dealing with hand pose estimation from video sequences, learning from sparse-labeled data is effective to reduce the burden of full annotations for video sequences, and the existing methods often leverage motion or photometric consistency as constraints between labeled and unlabeled frames [30], [31] to train models.

Since there is no large-scale real event-based hand dataset with 3D pose annotation, it motivates us to build a new real event-based hand dataset. In this work, we select multiple ubiquitous color cameras to get 3D hand pose annotations of event camera. However, due to the asynchronous imaging mechanism between color cameras and event cameras, the hand pose annotations from color cameras are very sparse relative to the temporally dense event streams. To deal with the sparse data annotation issue, we need to design effective constraints to enforce the predicted hand poses of the unlabeled frames to be feasible.

2.2 Event-based Pose Estimation

Since the events are mainly generated from the edge of the moving objects, when used for hand pose estimation, events can preserve the information of hand movement. A key problem for event-based hand pose estimation is to leverage edge and movement features for pose estimation.

Optical flow is an effective feature in event-based vision tasks, and it can serve as a useful approximation to hand motion fields when events are used for hand pose estimation. Although optical flow from event streams has been extensively studied [6], [32], [33], to the best of our knowledge, no existing work is specifically designed for hand motion. EV-FlowNet [32] learns self-supervised optical flow by photometric consistency of gray-scale images from the DAVIS camera [2], but it fails when capturing gray-scale images from fast motion or HDR scenes. To tackle this, Zhu *et al.* [33] learn an effective optical flow model in an unsupervised manner based on the contrast maximization method. However, it is still a open problem to estimate the hand specific optical flow (*hand flow*) by leveraging the hand shape model, and how to use hand flow to boost the hand pose estimation performance.

To utilize the edge information naturally encoded in events, EventCap [34] applies an edge fitting approach for human pose refinement which consists of two steps: 1) finding correspondences of events and mesh vertices, 2) minimizing the distance between events and 2D projections from corresponding vertices. Finding correspondences is the main challenge in the edge fitting procedure. EventCap [34] obtains the closest event for each boundary vertex in its closest event search, but this leads to two issues when tackling hand pose estimation task: 1) events are not aligned at the same time with the hand mesh, 2) fingers will gather together in optimization, and the optimization can be stuck in local minimum because an event may have several corresponding vertices. Thus, it is important to design effective edge constraints specially designed for hand. Incorporating the hand model into the estimated optical flow can effectively restore the hand motion process.

In the realm of pose estimation, event camera is firstly applied to human pose estimation. EventCap [34] utilizes initial pose estimation via gray-scale images to reconstruct high-frequency human pose motion by event trajectories. However, EventCap [34] requires additional gray-scale images (usually with generated qualities for scenes that events demonstrate advantages) as input, and could lead to unstable pose results under challenging illumination conditions or fast motions. EventHPE [35] estimates human pose from only event data, but predicting relative poses of neighboring event frames will lead to accumulated errors as time goes on.

When events are used for hand pose estimation, it is more challenging due to high degree-of-freedom hand motion, heavy self-occlusion and significant similarity between different hand parts. EventHands [9] is proposed to estimate 3D hand pose estimation from event streams. It estimates MANO parameters from Locally-Normalised Event Surfaces (LNES), which assigns higher weights to events close to the target timestamp and forms an event frame. However, it fails to resolve the motion ambiguity in pose estimation, *i.e.*, static hand parts will not trigger events, which leads to spatial uncertainty of these static parts. Jalees *et al.* [36] also propose a model-based approach to estimate 3D hand pose from event streams, which fits a hand model via nonlinear optimization and enforces event stream simulator to generate similar event frames to the real event camera. However, the hand tracking by optimization requires good initialization, and it is prone to be stuck at local minimum due to the non-convex optimization of the object function.

3 PRELIMINARIES

3.1 Hand Model Representation

We adopt a differentiable hand parametric MANO model [22], which can be formulated as:

$$M(\beta, \theta) = W(T_P(\beta, \theta), J(\beta), \theta, \mathcal{W}), \quad (1)$$

where a skinning function W (linear blend skinning [37]) is applied to an articulated rigged body mesh with shape T_P , joint locations J defining a kinematic tree, pose parameter θ , shape parameter β , and blend weights \mathcal{W} . Given pose and shape parameters, MANO model outputs a hand mesh with 778 vertices $\mathbf{v} = M(\beta, \theta) \in \mathbb{R}^{778 \times 3}$, and 3D joints $\mathbf{J}_{3D} \in \mathbb{R}^{21 \times 3}$ can be recovered by $\mathbf{J}_{3D} = J_{\text{reg}}(\beta, \theta)$, where J_{reg} is the regression function from the hand mesh and pose parameters to 3D joints. Hereafter, we denote $\varphi = (\beta, \theta)$ to be *hand parameters* for easy reference.

3.2 Image Formation and Motion Ambiguity

Event camera encodes the changes of per-pixel intensity $I(x, y, t)$ into event streams. An event $e_i = (x_i, y_i, t_i, p_i)$ is triggered at pixel (x_i, y_i) at time t_i when the logarithmic radiance change reaches the threshold:

$$\log I(x_i, y_i, t_i) - \log I(x_i, y_i, t_p) = p_i C, \quad (2)$$

where t_p is the timestamp of the last event fired at pixel (x_i, y_i) , $p_i \in \{-1, 1\}$ is the polarity of intensity change, C is the contrast threshold.

Due to the differential imaging mechanism of the event camera, the static hand part will not generate events under constant lighting. Events E_{t_{n-1}, t_n} within time interval $[t_{n-1}, t_n]$ may correspond to multiple hand poses (we call it “motion ambiguity” in event-based hand pose problem), because the static hand parts can have multiple pose states and their relative pose changes reflected by events could look the same. Several efforts such as EventHPE [35] are conducted to predict relative pose $\Delta\theta_{t_n}$ between the current frame and the previous frame $\varphi_{t_{n-1}}$. However, these approaches can not resolve the motion ambiguity issue, because the relative poses are still affected by the absolute hand poses even if they generate the same event stream.

One way to alleviate the challenge is to encode the previous event data to assist in estimating the current hand pose, because event camera is more likely to record complete hand movements over a long interval. In this paper, we use a Conv-GRU [38] recurrent model to embed the previous sequence features. We divide the asynchronous event sequence into several sub-segments for hand pose prediction. Given an event stream segment ranging from t_0 to t_N , we split the segment into N sub-segments $\{[t_{i-1}, t_i]\}_{i=1}^N$ with the same duration. Each sub-segment of the event stream will be represented as event frame and event volume for hand pose estimation.

4 METHODS

As shown in Figure 2, EvHandPose pipeline consists of two main parts: Event-to-Pose module and Pose-to-IWE (Image with Warped Events) module. The Event-to-Pose module is designed to predict hand pose from the asynchronous event stream in Section 4.1. It represents the edge feature as LNES [9] and predicts the shape flow (*i.e.*, a new optical flow specially designed for hands) with the proposed FlowNet to explore motion information from the asynchronous event stream. After fusing the edge feature and shape flow by a feature encoder, a Conv-GRU model is applied to alleviate the motion ambiguity issue by involving the temporal correlation between the neighboring event frames. The Pose-to-IWE module is then designed to supervise Event-to-Pose module during training. The key idea is to use the sparse annotations of hand shapes and hand joints as supervision when they are available, use a contrast maximization loss and edge loss on the unannotated event frames to enhance hand pose estimation performance, and use hand flow loss for all event frames. In Section 4.2, we elaborate on the details of these loss functions for annotated and unannotated event frames, respectively.

4.1 Motion Representations

Events in time interval $[t_{n-1}, t_n]$ contains two types of hand motion aware information (*i.e.*, optical flow and edge) under photometric consistency assumption. By recording the brightness

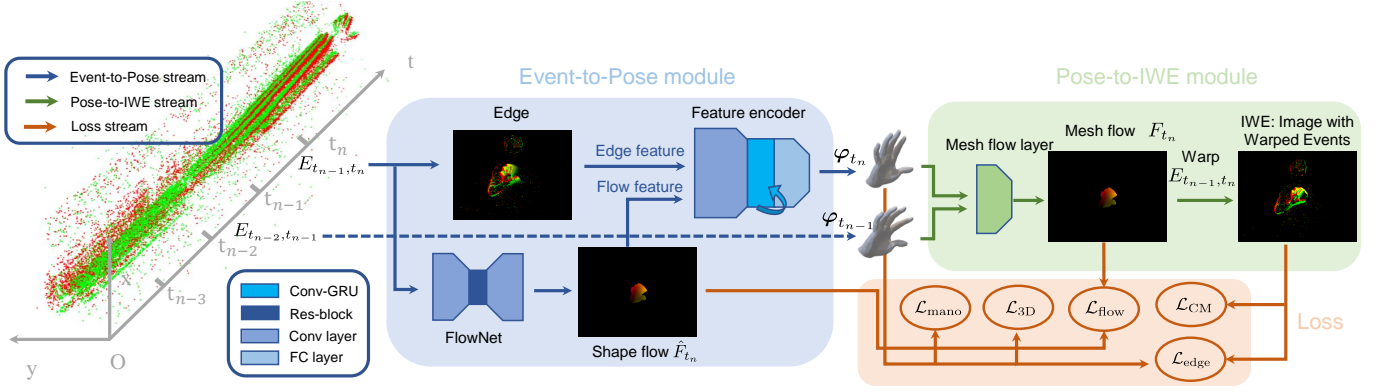


Fig. 2: Overview of EvHandPose pipeline. Event streams are firstly splitted into several sub-segments $\{E_{t_{k-1}, t_k}\}$, and they are represented as event frames and volumes. Event-to-Pose module extracts edge of each frame and shape flow \hat{F}_{t_n} of each volume by FlowNet, and predicts the hand parameters φ_{t_n} of the current event timestamp. Given sparsely annotated and unannotated event frames, we learn the hand pose estimation model by designing several self-supervised loss functions. Specially, we design a differential mesh flow layer (details in Figure 3) in Pose-to-IWE module to compute mesh flow F_{t_n} with the neighboring hand parameters φ_{t_n} and $\varphi_{t_{n-1}}$. In order to address the issue of sparse annotation, we warp the events in E_{t_{n-1}, t_n} with estimated hand flow to get IWE, and adopt contrast maximization loss and edge loss upon IWE for self-supervision. In the 2D visualization of events in this paper, red pixels represent positive events, green pixels represent negative events, and yellow pixels represent both types of events.

difference between the hand and background, events in $[t_{n-1}, t_n]$ describe the hand movement and can be used to resolve the motion ambiguity issue of hand pose estimation by including observations from previous status, and events at a specific timestamp t_n indicates the accurate hand edges. Therefore, we propose new motion representations that include both hand flow and edge information for event-based hand pose estimation.

As edges are naturally encoded in events, we utilize the edge information in Event-to-Pose module for accurate pose estimation. Specifically, we follow EventHands [9] to use the effective 2D representation LNES. The LNES image I is updated by iterating each event e_i in E_{t_{n-1}, t_n} :

$$I(x_i, y_i, p_i) = \frac{t_i - t_{n-1}}{t_n - t_{n-1}}. \quad (3)$$

The LNES can reserve the latest event information because it will be overwritten when an event with the same polarity occurs at that location.

4.1.1 Hand Flow from Events

We use two types of representation of hand flow from events. The first type is the model-based hand flow F (denoted as *mesh flow*) by designing differential hand flow layer with the neighboring hand parameters φ_{t_n} and $\varphi_{t_{n-1}}$. The second type of hand flow \hat{F} (denoted as *shape flow*) is obtained by the optical flow predicted by proposing a FlowNet (bottom right of Event-to-Pose module in Figure 2), which is learned using mesh flow as supervision.¹

Mesh Flow. Desired motion representations for event-based hand modeling should precisely describe the hand movement and ignore disturbance from the background. To achieve this, we calculate the dense hand flow by projecting two sequential MANO meshes on the image, and compute the displacements of corresponding vertices like [35] and [31].

Figure 3 illustrates hand flow computation process. Given two MANO models $M(\beta_{t_{n-1}}, \theta_{t_{n-1}})$ and $M(\beta_{t_n}, \theta_{t_n})$ at two event moments, we get $K + 1$ hand shapes $\{M_k\}_{k=0}^K$ with hand parameters $\{\varphi_k\}_{k=0}^K$ by linear interpolation of the hand parameters of the two MANO models as follows:

$$t_k = (1 - \frac{k}{K}) \cdot t_{n-1} + \frac{k}{K} \cdot t_n, \quad k = 0, 1, \dots, K. \quad (4)$$

$$\beta_k = (1 - \frac{k}{K}) \cdot \beta_{t_{n-1}} + \frac{k}{K} \cdot \beta_{t_n}, \quad k = 0, 1, \dots, K. \quad (5)$$

$$\theta_k = \text{slerp}(\theta_{t_{n-1}}, \theta_{t_n}, \frac{k}{K}), \quad k = 0, 1, \dots, K. \quad (6)$$

where spherical linear interpolation (*i.e.*, $\text{slerp}(\cdot)$) is used for pose parameters θ , and $\varphi_k = (\theta_k, \beta_k, t_k)$ is the interpolated MANO parameters at time t_k .

For each interpolated hand mesh M_k , we can compute the speed $\mathbf{S}_k \in \mathbb{R}^{778 \times 2}$ of all vertices of the hand mesh on the image as follows:

$$\mathbf{S}_{k,i} = \frac{K \cdot \pi(\mathbf{v}_{K,i} - \mathbf{v}_{k,i})}{(K - k) \cdot (t_n - t_{n-1})}, \quad k = 0, 1, 2, \dots, K-1, \quad (7)$$

where $\mathbf{v}_{k,i}$ is the i -th vertex on the hand mesh M_k , and π is the camera projection matrix.

Since the hand mesh represented by MANO model is a triangular mesh with 778 vertices, the displacements of the corresponding vertices of neighboring interpolated hand mesh M_k can not get dense optical flow. In order to deal with this issue, we get the corresponding triangle of each pixel (x, y) by the first intersection of the ray from the camera optical center to the pixel (x, y) and the hand mesh, and calculate the barycentric coordinates $b_{\mathbf{v}_j}(x, y)$ of the pixel (x, y) . Then we can compute the dense optical flow by the weighted sum of the vertex speed \mathbf{S}_k with barycentric weights $b_{\mathbf{v}_j}$ as follows:

$$F_k(x, y) = \sum_{\mathbf{v}_j \in V_{\text{bary}}(x, y)} b_{\mathbf{v}_j}(x, y) \mathbf{S}_{k,j}, \quad (8)$$

1. Please refer to Appendix A in the supplemental material for qualitative and quantitative comparisons of different flow representations.

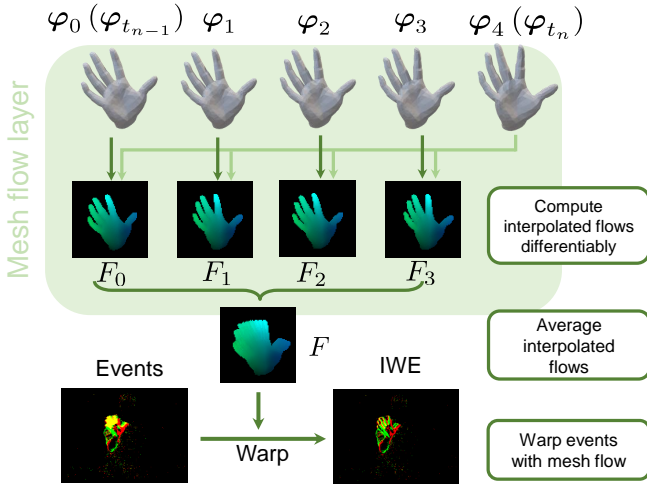


Fig. 3: Illustration of Pose-to-IWE module. Given MANO parameters $\varphi_{t_{n-1}}$ and φ_{t_n} , we first conduct interpolation to get interpolated MANO parameters $\{\varphi_k | k = 0, 1, \dots, K\}$, $K = 4$ here. Then we compute the interpolated flows $\{F_k\}$ by projecting the movements between each hand mesh $M_k (k = 0, 1, \dots, K - 1)$ and the last hand mesh M_K to the image plane. Lastly, we average all the interpolated flows to get the final hand mesh flow F .

where $V_{\text{bary}}(x, y)$ is the vertices of the corresponding triangle of pixel (x, y) . Then our mesh flow representation $F(x, y)$, which is differentiable with respect to hand parameters, is calculated as:

$$F(x, y) = \frac{\sum_{k=0}^{K-1} F_k(x, y)}{\sum_{k=0}^{K-1} \mathbb{1}(F_k(x, y))}, \quad (9)$$

where $\mathbb{1}$ is the function to indicate whether there is flow at pixel (x, y) . Events are mainly triggered from the edge of the hand under constant lighting condition. If we warp a period of events to a certain timestamp, events from the same position on the hand will gather together to form sharp hand edges and accumulated an image with warped events. As shown in Figure 3, IWEs by our mesh flow have sharp edges, which will serve for the contrast maximization and edge constraints in our self-supervision framework.

Shape Flow. While mesh flow is obtained from the hand model and serves for self-supervision losses, Event-to-Pose module needs to directly extract motion information from event streams for accurate hand pose estimation. Thus Event-to-Pose module uses FlowNet which is a U-Net like CNN backbone to predict hand shape flow from event volumes [33]. Being different from [33], our FlowNet is supervised by mesh flow and only learns hand movement information, not background movement information, thus reserving high quality hand movement information. We apply the endpoint error (EPE) between shape flow \hat{F}_{t_n} and mesh flow F_{t_n} as loss function, which is the normal measurement for optical flow estimation:

$$\mathcal{L}_{\text{flow}} = \sum_n \text{EPE}(\hat{F}_{t_n}, F_{t_n}). \quad (10)$$

4.2 Self-supervised Learning Framework

The annotations are only available for sparse subset of event frames, because the annotations are provided with sparse frames of multiple color cameras (details in Section 5). In this section, we formulate

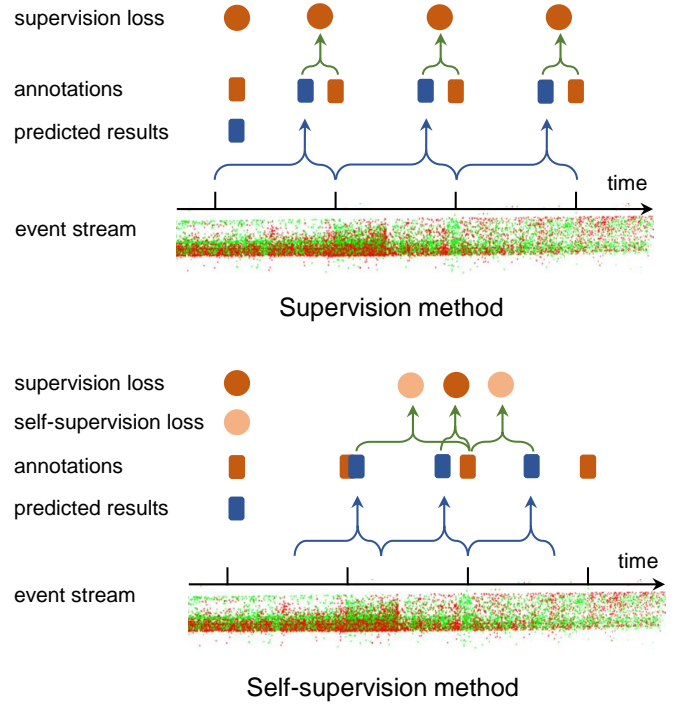


Fig. 4: Comparison of supervision and self-supervision methods. In supervision method, the model can only learn hand poses at annotated timestamps and the interval of each event sub-segment has to be strictly overlapped with the annotated period. In self-supervision method, we only need partial labels and the outputs of unlabeled sub-segments are constrained by self-supervision loss. Therefore, EvHandPose can learn hand poses at any timestamp near the annotations with dynamic time window for event sub-segment representation.

the self-supervised framework that can learn the hand pose model using both the sparse annotated and unannotated event frames.

4.2.1 Learning under Sparse Annotations

Event-to-Pose module of EvHandPose extracts edge feature and hand flow from event streams, and predicts the hand MANO parameters. When annotations of 3D joints and hand MANO parameters are available, we use 3D joint loss \mathcal{L}_{3D} and hand MANO parameter loss $\mathcal{L}_{\text{mano}}$ for model learning:

$$\mathcal{L}_{3D} = \sum_n \|J_{\text{reg}}(\hat{\beta}_n, \hat{\theta}_n) - \mathbf{J}_{3D_n}\|^2, \quad (11)$$

$$\mathcal{L}_{\text{mano}} = \sum_n (\lambda_\beta \|\hat{\beta}_n - \beta_n\|^2 + \lambda_\theta \|\hat{\theta}_n - \theta_n\|^2), \quad (12)$$

where \mathbf{J}_{3D_n} is the ground-truth 3D joints vector, MANO parameters with hat ($\hat{\beta}, \hat{\theta}$) are prediction results and those without hat (β, θ) are ground-truth, λ_β and λ_θ are loss weights and they are set to 0.25 and 5.0, respectively.

Therefore, the loss function $\mathcal{L}_{\text{super}}$ to learn under supervision can be formulated as follows:

$$\mathcal{L}_{\text{super}} = \lambda_{3D} \mathcal{L}_{3D} + \lambda_{\text{mano}} \mathcal{L}_{\text{mano}}, \quad (13)$$

where λ_{3D} and λ_{mano} are loss weights, and they are set to 1000 and 0.1 in our experiments, respectively.

4.2.2 Learning with Self-supervision

Since we get the annotated hand pose dataset EvRealHands using multiple RGB cameras, hand pose can be annotated at a pre-defined fps (e.g., 15 fps in EvRealHands). Due to the asynchronous image mechanism of event camera, the event streams can only have sparse hand pose annotations. In order to supervise the unannotated event sub-segment and leverage the dense event streams, we propose a self-supervised framework to effectively utilize the event with sparse annotations as shown in Figure 4. Specially, we design a contrast maximization loss to constrain the movement of the hand over time, and an edge loss to learn hand pose at predicted time, and adopt smooth loss to encourage the smoothness of the sequential predicted hand poses.

Contrast Maximization Loss. Inspired by the contrast maximization method that was originally proposed to handle motion compensation problem [39], we design a new contrast maximization loss (denoted as CM loss) for self-supervision. The key idea of CM loss is to enforce the IWE is sharp and has good contrast, an effective global statistical priors of IWE.

Event-to-Pose module can predict sequential hand MANO parameters $\{\varphi_{t_n} | n = 1, \dots, N\}$. For each neighboring pair of parameters $\{\varphi_{t_{n-1}}, \varphi_{t_n}\}$, we can compute the mesh flow F_n , and warp the events in $[t_{n-1}, t_n]$ to get the image with warped events $IWE_{n,\hat{t}}$ at timestamp \hat{t} as follows:

$$IWE_{n,\hat{t}} = \text{Warp}(E_{t_{n-1},t_n}; F_n; \hat{t}), \quad (14)$$

where $\text{Warp}(\cdot, \cdot, \cdot)$ is the function to warp events with mesh flow.

Then we use the focus loss functions using variance measure in [40] to evaluate how well events are aligned along the hand flow, i.e., the contrast of the image with warped event, as follow:

$$\text{Var}(I) = \frac{1}{N_I} \sum_{i,j} (h_{ij} - \mu_I)^2, \quad (15)$$

where N_I is the number of pixels of image I , and $\mu_I = \frac{1}{N_I} \sum_{i,j} h_{ij}$ is the mean value of image I .

The CM loss is finally defined by computing the contrasts in both forward and backward direction as follows:

$$\mathcal{L}_{\text{CM}} = - \sum_n (\text{Var}(IWE_{n,t_n}) + \text{Var}(IWE_{n,t_{n-1}})), \quad (16)$$

where IWE_{n,t_n} and $IWE_{n,t_{n-1}}$ are the forward and backward IWEs at timestamp t_n and t_{n-1} , respectively.

Edge Loss. As shown in Figure 3, IWE should demonstrate sharp hand edges, and this inspires us to design an edge loss to enforce the alignment of the projection of predicted hand shape and the edge of IWE. Intuitively, such a constraint can bring a benefit that the local details of the reconstructed hand shape are well consistent to the event observation. However, it is challenging to find reliable correspondences of events and hand mesh vertices due to two issues: 1) Events are not aligned at the same time with the hand shape and 2) fingers will gather together in optimization because an event may have several corresponding vertices.²

To solve the above misalignment issues, we first warp the events in $[t_{n-1}, t_n]$ by mesh flow and get IWE at timestamp t_n . We then find the correspondence between pixels of IWE and hand mesh vertices by searching the proper hand vertex for each IWE pixel. In order to reduce computation cost and make our method robust

to noisy events, we only select M IWE key pixels with the most accumulated events to calculate the edge loss. For each key pixel $IWE(x_i, y_i)$, we get a candidate set of hand mesh vertices P_i that can be projected within a local neighborhood of the pixel (x_i, y_i) (e.g., 12×12). For these vertices, we select a candidate vertex using both orientation weight w_j^o and motion weight w_j^m .

Since hand mesh vertices with the normal vectors perpendicular to the camera ray will generate more events, we design the orientation weight to each vertex \mathbf{v}_j as follows:

$$w_j^o = b_{\text{orient}} - \|\cos(\mathbf{n}_j, \mathbf{d}_j)\|, \quad (17)$$

where \mathbf{n}_j is the normal vector at \mathbf{v}_j , \mathbf{d}_j is the camera ray pointing from the camera center to \mathbf{v}_j , and $b_{\text{orient}} = 1.2$ is a constant weight bias.

We further observe that vertices with large motion displacements often produce more events, so we design the motion weight of vertex \mathbf{v}_j as follows:

$$w_j^m = \sqrt{\|\pi(\mathbf{v}_{j,t_{n-1}}) - \pi(\mathbf{v}_{j,t_n})\|^2 + b_{\text{motion}}}, \quad (18)$$

where $\pi(\cdot)$ is the projection function, $\mathbf{v}_{j,t_{n-1}}$ is the vertex at timestamp t_{n-1} , and $b_{\text{motion}} = 4.0$ is the constant weight bias.

Next, we design a metric $\text{metric}_{i,j}$ with the orientation weight w_j^o and the motion weight w_j^m , and select the corresponding vertex \mathbf{v}_{P_i} of $IWE(x_i, y_i)$ with the highest metric value. Such a metric can be defined as:

$$\text{metric}_{i,j} = \frac{w_j^o \cdot w_j^m}{\|\pi(\mathbf{v}_{j,t_n}) - IWE(x_i, y_i)\|^2 + b_d}, \quad (19)$$

where $b_d = 4.0$ is the constant shift of distance.

The edge loss is finally defined as :

$$\mathcal{L}_{\text{edge}} = \sum_n \frac{\sum_i^M w_{P_i}^o \cdot w_{P_i}^m \cdot \|\pi(\mathbf{v}_{P_i,t_n}) - IWE(x_i, y_i)\|^2}{\sum_i^M w_{P_i}^o \cdot w_{P_i}^m}. \quad (20)$$

Smooth Loss. To ensure the smoothness of the predicted hand parameters of event streams, we use a smooth loss $\mathcal{L}_{\text{smooth}}$:

$$\mathcal{L}_{\text{smooth}} = \sum_n \text{sigmoid}(\max(0, \lambda_\beta \|\hat{\beta}_n - \hat{\beta}_{n-1}\|^2 + \lambda_\theta \|\hat{\theta}_n - \hat{\theta}_{n-1}\|^2 - b_{\text{smooth}})), \quad (21)$$

where the sigmoid function is used to avoid the gradients of $\mathcal{L}_{\text{smooth}}$ to be large, $b_{\text{smooth}} = 0.5$ is the empirical margin of the smooth loss, and the hyper-parameters λ_β and λ_θ are set to 0.2 and 1.0, respectively.

In summary, the predicted results from the Event-to-Pose module are fed into the Pose-to-IWE module. Those results of the unlabeled segments will be constrained by the self-supervision loss $\mathcal{L}_{\text{self}}$:

$$\mathcal{L}_{\text{self}} = \lambda_{\text{CM}} \mathcal{L}_{\text{CM}} + \lambda_{\text{edge}} \mathcal{L}_{\text{edge}} + \lambda_{\text{smooth}} \mathcal{L}_{\text{smooth}}, \quad (22)$$

where λ_{CM} , λ_{smooth} , and λ_{edge} are loss weights, and they are set to 3, 0.1, 0.2, respectively.

4.2.3 Training Strategy

Our training strategy consists of three steps. First, we train FlowNet under supervision with $\mathcal{L}_{\text{flow}}$ and fix its parameters in the following steps. Then, we train EvHandPose under supervision with $\mathcal{L}_{\text{super}}$ to get reasonable good parameter initialization. Finally, we train EvHandPose with both labeled data and unlabeled data with \mathcal{L}_{all} ,

² Please refer to Appendix B in the supplemental material for qualitative and quantitative comparisons of different edge losses.

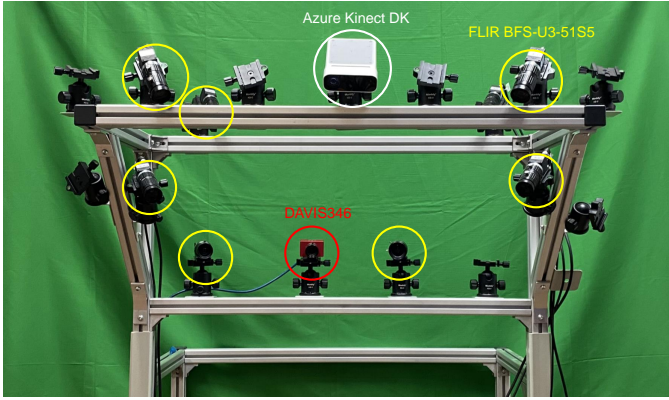


Fig. 5: Multi-camera system for hand data acquisition and annotation for creating EvRealHands dataset. Seven FLIR BFS-U3-51S5 cameras (yellow) are synchronized to capture multi-view RGB images and the event camera DAVIS346 (red) captures the event streams. We also attach an Azure Kinect DK (white) as an auxiliary camera to use the depth image only for accurate geometric calibration of the camera system.

which contains supervision loss and self-supervision loss and can be formulated as follows:

$$\mathcal{L}_{\text{all}} = \lambda_{\text{super}}\mathcal{L}_{\text{super}} + \lambda_{\text{self}}\mathcal{L}_{\text{self}}, \quad (23)$$

where λ_{super} and λ_{self} are weighting factors, and set to 2.0, 1.0.

5 DATASET

We present the first real-world event-based hand pose dataset EvRealHands. Our dataset contains event streams and RGB image with annotations of 3D hand pose and hand shape parameter, and it contains hand poses of commonly used hand gestures. EvRealHands is collected under common scenarios (*e.g.*, normal lighting and hand movements) and challenging scenarios such as strong light, flash and fast motion scenes, which are overlooked in previous hand pose datasets as shown in Table 1.

5.1 Data Acquisition

Capture System Setup. EvRealHands is captured in a multi-camera fashion similar to [41] and [42]. As shown in Figure 5, the multi-camera system consists of 7 RGB cameras (FLIR, 2660×2300 pixels) and an event camera (DAVIS346, 346×260 pixels). We synchronize all the cameras with an external TTL signal of 15 Hz. For calibration, we use a moving calibration chessboard and calculate the intrinsic and extrinsic parameters following [43] with RGB frames from FLIR, APS frames from DAVIS346 and depth frames from an auxiliary RGB-D camera (Azure Kinect DK). The average pixel root mean square error on all the images in calibration reaches 0.184.

Hand Gestures. We collect 84 sequences from 10 subjects with duration ranging from 20 s to 60 s as summarized in Table 2.³ For each subject, we collect 3 sequences for each hand under normal lighting, which consists of 15 pre-defined hand poses shown in Figure 6 similar to [44] about 40 s (fixed poses), random hand poses about 20 s (random short), random hand poses about 60 s

3. Please refer to Appendix C in the supplemental material for assessing the adequacy of EvRealHands.

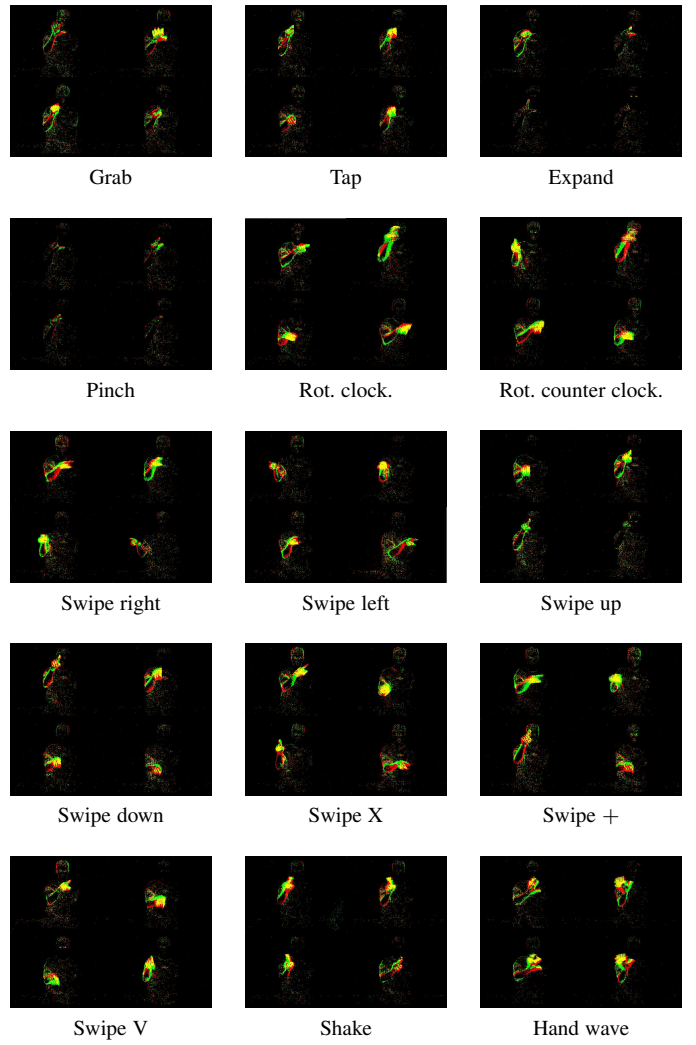


Fig. 6: Illustration of the 15 fixed pose gestures in event frames (“Rot.” and “clock.” are short for rotation and clockwise).

(random long). As shown in Figure 7, the hand pose variance in random pose sequences is larger than that in fixed pose sequences.

Scenes with Challenging Illuminations and Motions. We also capture 12 sequences for strong light scenes and 8 sequences for flash scenes from 2 subjects. We utilize two glare flashlights with 2000 lumen. We keep the flashlights on in strong light scenes and make the flashlights flash at a rate of 1 Hz in flash scenes to capture the event streams. Simultaneously, we keep the annotation RGB cameras from overexposure by reducing their exposure time. We also collect 4 fast motion sequences from 2 subjects.

5.2 Annotation

5.2.1 3D Joint Annotation

Our dataset is of single hands and we apply 21 keypoints scheme [12] to annotate each hand. Inspired by Interhand2.6M [45] and FreiHand [46], we use multi-view RGB images for 3D annotation and apply a two-stage process consisting of machine annotation and human annotation. First, we use Mediapipe [47] to detect 2D hand keypoints on all the RGB images and triangulate 2D keypoints to obtain 3D keypoints with RANSAC method. Then we manually verify all the keypoints re-projected by 3D keypoints

TABLE 1: Comparison of existing event-based hand pose estimation dataset and EvRealHands. EvRealHands involves multiple real-world challenging scenes. We measure the amount of event data by their sequence length.

Dataset	Source	Type	Resolution	Subjects	Annotation			Scenes	
					Method	3D joints	Strong light	Fast motion	Flash
EventHands [9]	Event	Synthetic	240 × 180	1	Synthetic	1.24 M	None	12.6 s	None
EvRealHands	Event + RGB	Real	346 × 260	10	Human+machine	59.3 K	456.5 s	69.2 s	316.7 s

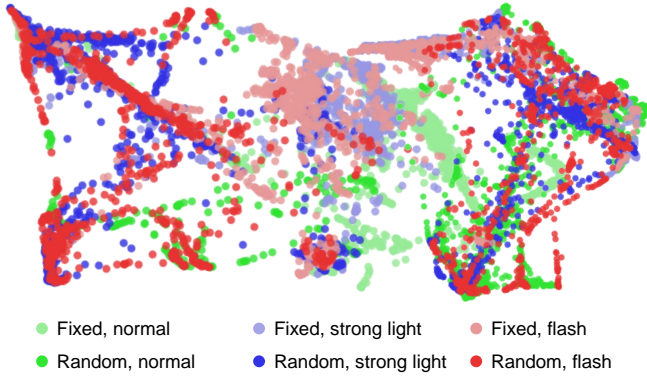


Fig. 7: Visualization of hand pose distribution on different scenes using t-SNE. In our visualization setup, each vector fed into t-SNE is MANO hand pose parameters with 48 dimension. The metric for t-SNE is the geodesic distance in $SO(3)$ between the two rotation vectors. It is obvious that random poses have a larger variance than fixed poses.

TABLE 2: Detailed attributes of EvRealHands. The duration of event streams, the quantity of RGB images, and their annotations in each scene are shown below. Annotations [mc] means the 3D annotations are checked or annotated manually, while Annotations [all] refer to all the machine and manual annotations. For fast motion sequences, the annotations are 2D keypoints.

Data	Normal		Strong light		Flash		Fast motion
	Fixed	Random	Fixed	Random	Fixed	Random	
Event streams (s)	850.7	2759.0	150.3	306.2	158.8	157.9	69.2
RGB images	79.7 K	265.8 K	14.2 K	27.4 K	14.9 K	13.8 K	5.2 K
Annotations [mc]	11.4 K	9.7 K	2.0 K	1.9 K	2.1 K	1.9 K	0.8 K
Annotations [all]	11.4 K	37.2 K	2.0 K	3.9 K	2.1 K	1.9 K	0.8 K

and select the unqualified views for human annotation. Since our annotations have been checked manually, we do not perform a bootstrapping procedure as [41]. Due to the cost of human annotation, manual annotation is only applied to fixed pose and random short sequences and machine annotation is then applied to random long sequences. For fast motion sequences, we can not get accurate 3D joint annotations due to the severe motion blur in the captured images. To quantitatively evaluate our method, we manually annotate the 2D joints on the event sequences.

5.2.2 Shape Annotation

We use MANO shape parameter β to represent the hand shape. We first scan the hands of each subject with an Artec Eva 3D Scanner, and get meshes of static hands shown in Figure 8. Then we fit a hand MANO model to each mesh to get the prior shape parameter. For each frame of multiple RGB cameras, we fit hand MANO parameters with prior shape as initialization under the constraints

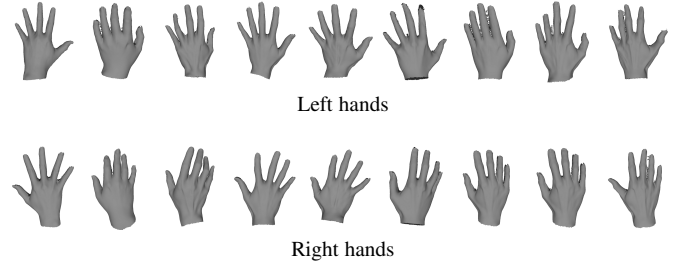


Fig. 8: Scanned hand meshes. We use 3D scanner to get precise hand mesh for shape annotation.

from 2D keypoints, 3D joints, and regularization terms similar to FreiHand [46].

6 EXPERIMENTS

In this section, we will first introduce the experiment setup including dataset and evaluation metrics in Section 6.1 and implementation details in Section 6.2. Then we will compare our method with baselines on different scenes in Section 6.3. ⁴ Finally, we will perform ablation study to demonstrate the claimed effect of each component we propose in Section 6.4.

6.1 Dataset and Evaluation Metrics

6.1.1 Training and Evaluation Data

We collect sequences from 7 out of 10 subjects as training data, 1 as validation data, and 2 as evaluation data. The training data included about 4 minutes of strong light sequences, 2 minutes of flash sequences, and no fast motion data. The evaluation data included 8 sequences under normal scenes, 4 sequences of strong light, 4 sequences of flash, and 2 sequences of fast motion. In the sequences mentioned above, the left and right hands are equally divided. In our training process, we flip the left hand data into the right hand for increasing the amount of data.

6.1.2 Evaluation Metrics

Similar to previous evaluation metrics [9] and [16], we apply root-aligned mean per joint position error (MPJPE) in mm and the area under the curve (AUC) of PCK (percentage of correct keypoints) with thresholds ranging from 0 to 10 cm for 3D annotated sequences. For fast motion sequences, we do not have 3D annotations. We compute root-aligned 2D-MPJPE (pixels) on keypoints which have been normalized by the palm length (distance from wrist to MCP joint) as evaluation metric. Since our 2D joint annotations are on the imaging plane of the event camera, the 3D joints predicted by the RGB-based approach are projected onto the imaging plane of the event camera for evaluation.

4. Please refer to our supplemental video for more results.

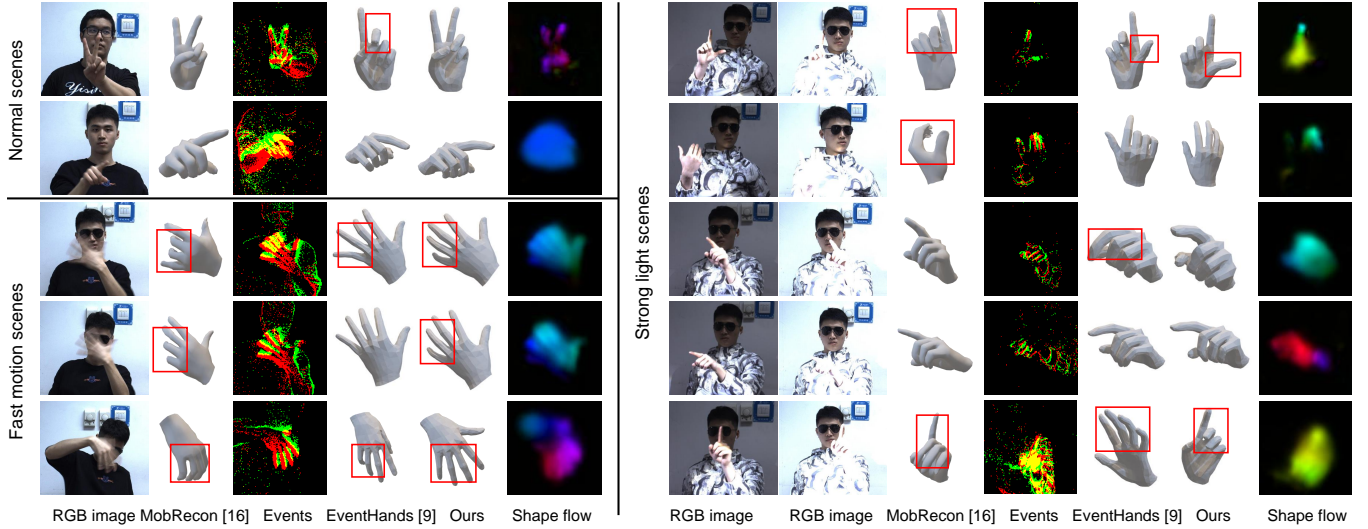


Fig. 9: Qualitative analysis. Left top two rows: normal scenes, left bottom three rows: fast motion scenes, right rows: strong light scenes. Columns from left to right: RGB images, poses from MobRecon [16], event frames, poses from EventHands [9], poses from EvHandPose (ours), shape flows. In order to see the hands more clearly, we add normally exposed RGBs image to the left of the strong light scenes. EvHandPose achieves accurate and robust hand pose estimation compared with EventHands [9] and MobRecon [16] as highlighted in red boxes.

6.2 Implementation Details

Since we use temporal information through recurrent model, we need to divide an event stream into N sub-segments. In our experiment, N is 12, and we utilize the outputs of the last three sub-segments for supervision. For supervision, the interval of each sub-segment is 66.66 ms, which is the same with the period of annotations. For self-supervision, we only let second last sub-segment have 3D annotation, so that we can dynamically choose the interval of the sub-segment and the model can learn more hand information with different intervals. For the sub-segment with annotation, we use its ground truth hand pose instead of predicted hand pose in Pose-to-IWE module. The interval is randomly selected from 10 ms to 100 ms for self-supervision. Certainly, all the sub-segments have the same duration in a sequence. For evaluation, we set the interval of each sub-segment to 5 ms for fast motion sequences and 66.66 ms for other sequences.

In order to make the network effectively extract the feature of the hand, we calculate a bounding box for each sub-segment and then crop out the events inside this bounding box. Obtaining a bounding box for a event sub-segment is different from the RGB image due to the different temporal distributions. Given 3D joints at some timestamp, we project them onto the image plane to obtain the 2D joints and cover the 2D joints with an exact rectangle. We set the square with the center of the rectangle and 1.5 times the length of the longest side of the rectangle as bounding box. To compute a bounding box for a event sub-segment, we first approximately estimate the 3D joints of the start time and end time of this sub-segment with quadratic interpolation. Then we calculate the bounding boxes of the 3D joints and apply a bounding box that covers the two bounding boxes exactly as the final bounding box. For fast motion sequences, our machine annotated 3D joints are not very precise. We apply annotated 2D joints interpolation for generating bounding boxes.

We apply data augmentation including scale, rotation, and translation on events and resize the cropped event frames to

128×128. We use ResNet34 [48] as the backbone of feature encoders, and apply Adam [49] as the optimizer for all our training procedures. The learning rate of FlowNet and EvHandPose in supervision is 0.0005 and for EvHandPose in self-supervision is 0.0001. We train EvHandPose on two TITAN RTX GPUs with batch size 32.

6.3 Comparison with State-of-the-art Methods

6.3.1 Baselines

In order to compare the hand pose estimation performance of event camera and RGB camera under challenging scenes, we select MobRecon [16] as the baseline, because MobRecon [16] can achieve the state-of-the-art results on popular RGB datasets such as FreiHAND [46], *etc.* To compare with the most relevant solutions, *i.e.*, event-based hand pose estimation methods, we select EventHands [9], the first neural event-based 3D hand pose estimation approach, which demonstrates better performance than RGB-based methods on their proposed synthetic dataset. For MobRecon [16], we select the data of one viewpoint from our camera acquisition system and divide the dataset according to the above convention for the sake of fairness. We use the officially released codes of EventHands and MobRecon for comparison.

6.3.2 Results

In this section, we compare the state-of-the-art color-based and event-based hand pose methods, *i.e.*, MobRecon [16] and EventHands [9], under different typical hand interaction scenarios including normal scenes, strong light scenes, and fast motion scenes. We show the results of different methods qualitatively and quantitatively in Figure 9, Figure 10, and Table 3, respectively. Quantitative results show that EvHandPose predicts more accurate hand pose than EventHands [9] by MPJPE 10 ~ 20 mm lower and AUC 0.1 ~ 0.18 higher. This is because our method leverages the temporal and spatial features of events effectively, and addresses the issues of motion ambiguity and sparse annotations. Compared

TABLE 3: Quantitative experiments results of different methods and ablation study results.

Scenes	Poses	Metrics	EventHands [9]	MobRecon [16]	EvHandPose (all)	EvHandPose (w/o edge)	EvHandPose (w/o CM)	EvHandPose (super)	EvHandPose (super, w/o flow)
Normal	Fixed	MPJPE	40.06	17.39	22.60	23.64	23.59	23.95	26.44
		AUC	0.609	0.817	0.774	0.768	0.767	0.763	0.736
	Random	MPJPE	53.19	17.34	33.81	33.49	34.36	34.66	37.83
		AUC	0.523	0.818	0.670	0.678	0.665	0.660	0.632
Fast motion	Random	2D-MPJPE	1.87	1.19	0.88	1.04	1.00	1.14	1.26
Strong light	Fixed	MPJPE	49.78	33.14	30.44	33.32	31.78	32.75	32.76
		AUC	0.519	0.657	0.696	0.681	0.684	0.674	0.673
	Random	MPJPE	57.33	47.19	38.81	37.03	38.69	38.62	41.22
		AUC	0.475	0.528	0.618	0.640	0.620	0.620	0.594
Flash	Fixed	MPJPE	57.00	24.94	36.36	36.62	38.21	39.40	37.22
		AUC	0.481	0.738	0.647	0.632	0.630	0.626	0.636
	Random	MPJPE	73.43	29.66	57.98	56.81	58.47	58.67	55.35
		AUC	0.388	0.690	0.493	0.482	0.490	0.492	0.488

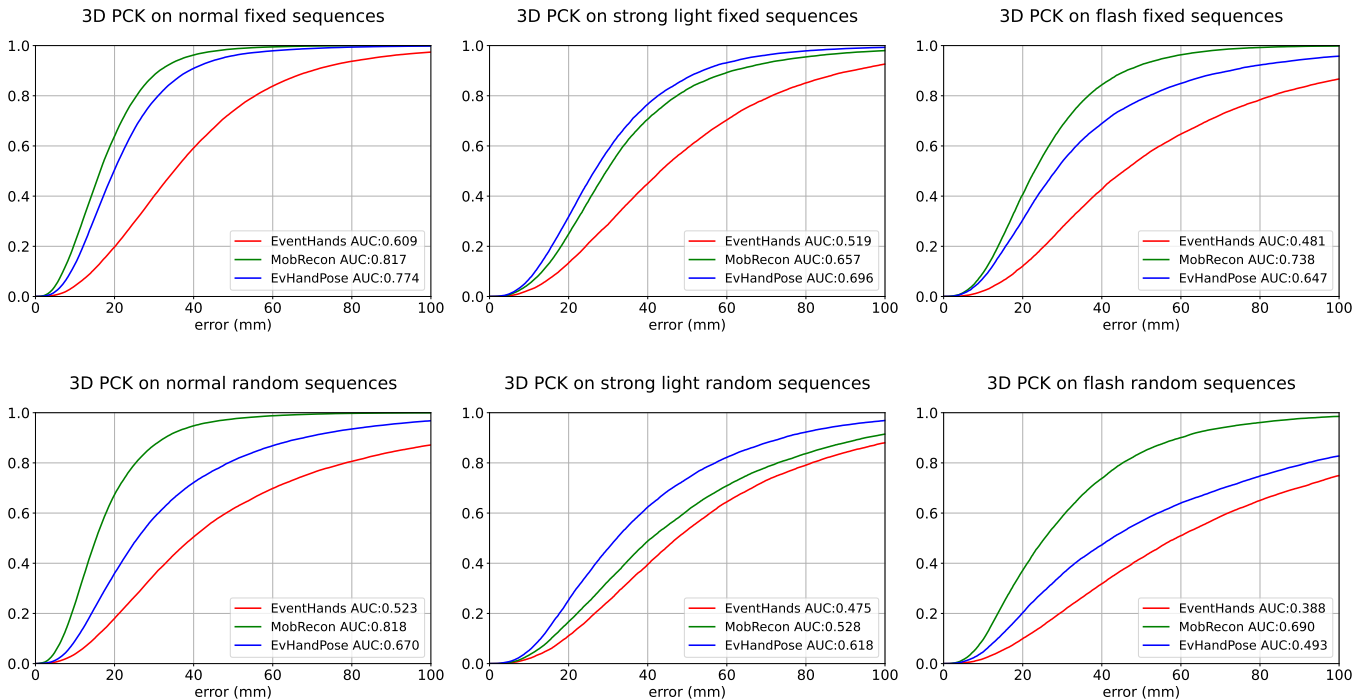


Fig. 10: 3D PCK curves of different methods on different scenes.

with the RGB method MobRecon [16], our method achieves better performance in challenging scenarios such as strong light and fast motions. In normal scenes, the performance of our method is slightly worse (but comparable) than MobRecon [16]. This is reasonable due to the significant higher spatial resolution and richer texture features of RGB images.

Normal Scenes. In normal scenes, our method outperforms EventHands [9] on MPJPE by 15 ~ 20 mm and AUC by 0.15 ~ 0.17. As shown in Figure 10 and Table 3, MPJPE of our method in the fixed pose sequences reaches 22.60 mm. As stated in Supanic *et al.* [50], human annotators could achieve an accuracy about 20 mm for hand, and can easily distinguish two poses if the error exceeds 50 mm. Therefore, our method can already achieve sufficient hand pose performance for practical gesture interaction applications. MobRecon [16] works better than our approach in

normal scenes, because it uses image input with significantly richer texture features and higher spatial resolutions.

Fast Motion Scenes. In fast motion sequences, EvHandPose outperforms EventHands with lower 2D-MPJPE. This is because in training procedure EvHandPose learns the optical flow generated by hand movement on the one hand, and the dynamic time window make EvHandPose more adaptable to sub-segments of different intervals. Compared to MobRecon [16], EvHandPose has a 2D-MPJPE performance gain of 26.05%. The main reasons for worse performance of MobRecon can be summarized as: Fast motion will lead to severe hand motion blur effect of RGB camera, and it is often infeasible for MobRecon [16] or human annotators to extract accurate hand region and keypoints from blurred images. However, the asynchronous imaging nature of the event camera allows it to capture microsecond motion information and EvHandPose adopts

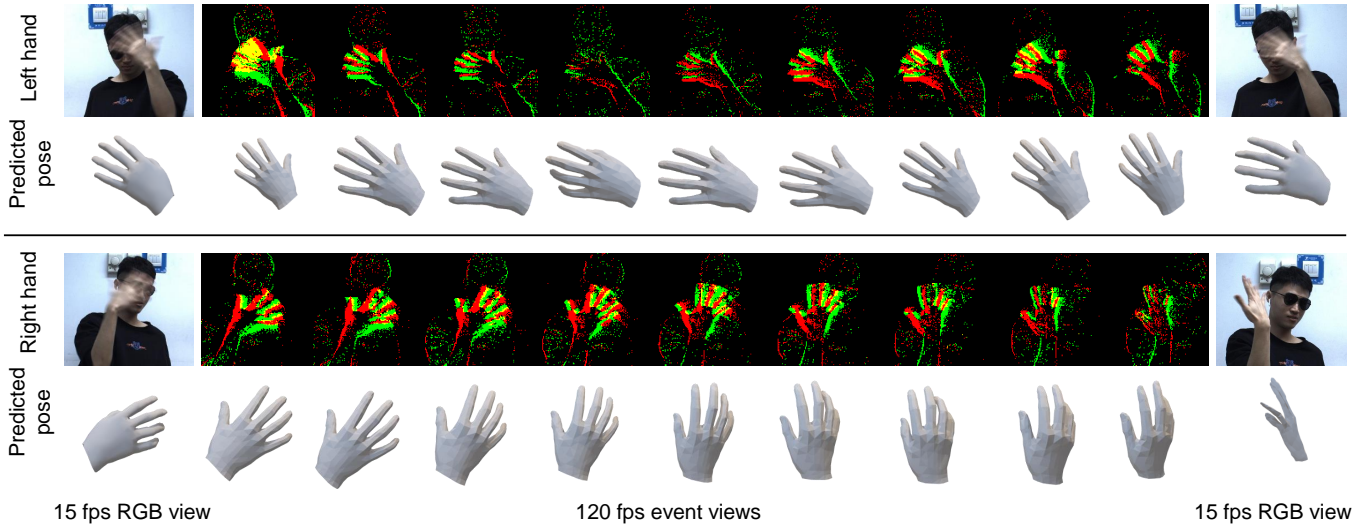


Fig. 11: Illustration of 120 fps event-based hand pose estimation. The two columns on the left and right end are neighboring RGB frames at 15 fps and their predicted hand poses by MobRecon [16]. The nine middle columns are the corresponding event frames and predicted poses by EvHandPose at 120 fps. EvHandPose achieves robust pose estimation compared with MobRecon [16] at much higher fps.

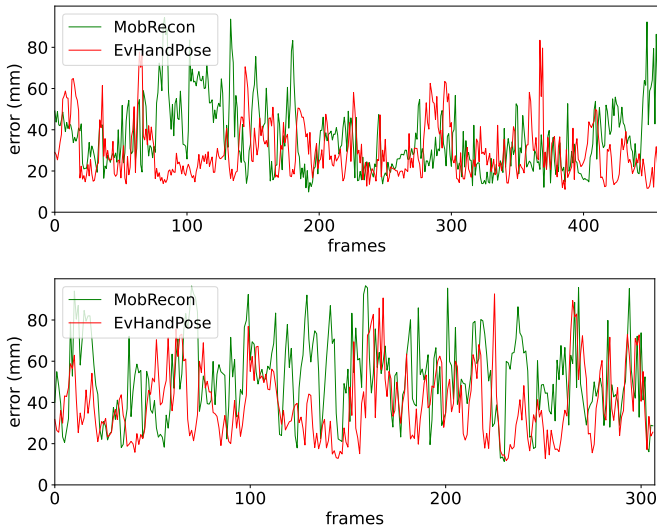


Fig. 12: Errors on two strong light sequences. Under strong light, EvHandPose has lower prediction error than MobRecon [16].

motion representations to record the hand movement precisely. The edge representation of the hand is still clear in event frames by setting the event time window to very short intervals (*e.g.*, 5 ms). The stable edge and motion representations enable EvHandPose to achieve accurate high fps hand pose estimation. Figure 11 shows the estimation of hand pose at 120 fps. Thus, our method can inspire future applications containing fast hand motions.

Strong Light Scenes. As shown in Figure 12, EvHandPose predicts more stable and accurate hand poses than MobRecon [16] on strong light sequences with MPJPE 3 ~ 10 mm lower and AUC 0.04 ~ 0.09 higher. As shown in Figure 9, under strong light, hand overexposure leads to loss of texture information, and it is challenging to estimate hand pose from overexposed images in RGB-based methods. However, EvHandPose can still extract edge and hand flow feature from the event stream under strong light, thus

achieving robust 3D hand pose estimation. It is worth mentioning that MobRecon [16] can still estimate hand pose from the mask of the hand when the hand is overexposed but the background still has texture features. This result shows that current RGB-based method have a strong ability to extract geometric information from images. As shown in Figure 9, EvHandPose involves hand motion information in Event-to-Pose module, which makes it more robust and accurate than EventHands [9]. EvHandPose has a 5 ~ 8 mm increase in MPJPE in strong light scenes compared to normal scenes. One reason is that the distribution of the events generated under strong light is different from that under normal scenes, even though they both record the edge motion. The other reason is that background and shadow of the hand under strong light will also produce a large number of events, making it hard to predict accurate hand poses.

6.4 Ablation Study

We conduct ablation studies on the contributed modules of our method. Specially, we evaluate the effect of the predicted hand flow on hand pose estimation, and the influence of used losses such as edge loss and CM loss in the self-supervised learning.

Effect of Predicted Hand Flow. As shown in Figure 9, EvHandPose predicts hand flow from events in its Event-to-Pose module. On the one hand, shape flow can alleviate motion ambiguity issue because it contains the temporal information of hand movements as shown in the first row of the results under strong light in Figure 9. On the other hand, hand shape flow can separate the hand from the background, thus improving the accuracy of estimation. Under supervised training, we compare the experimental results with and without hand flow, denote as EvHandPose (super) and EvHandPose (super, w/o flow). Under normal and strong light scenes, shape flow provides a 2 ~ 3 mm MPJPE decrease and a 0.02 ~ 0.03 AUC increase. On fast motion sequences, shape flow makes EvHandPose outperform MobRecon [16], which preliminarily verify the potential of the event camera on robust hand pose estimation.

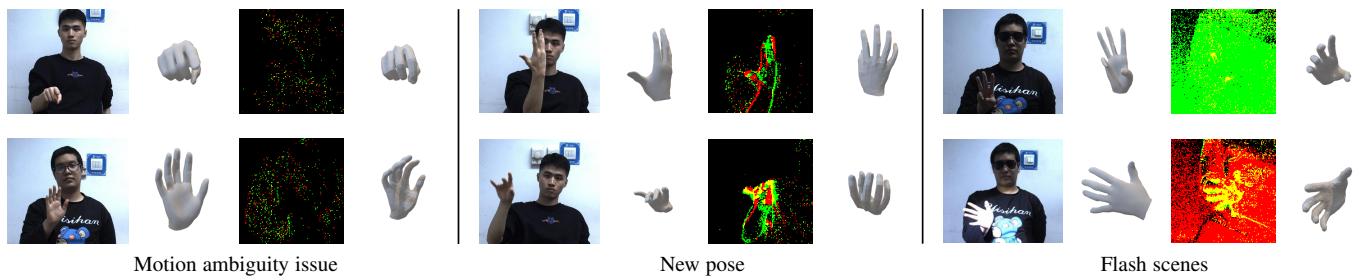


Fig. 13: Three kinds of failure cases: motion ambiguity issue, new pose, and flash scenes. From left to right for each picture combination: RGB view, hand pose from MobRecon [16], event frame, hand pose from EvHandPose.

Effect of Self-supervised Loss. We evaluate the influence of the self-supervised framework and each loss item on the performance of EvHandPose. In Table 3, EvHandPose (all), EvHandPose (w/o edge), and EvHandPose (w/o CM) respectively mean the complete loss, the methods of removing edge loss or CM loss. As shown in Table 3, compared with the EvHandPose under supervision, our self-supervised framework lead to a $1 \sim 2$ mm decrease in 3D-MPJPE in each scene, due to the effective usage of temporal dense event streams. Especially for fast motion sequences, our 2D-MPJPE reduced by 22.8% compared with the supervision method. According to the experiments, both losses contribute to the performance on the fast motion scenes. CM loss improves the performance on random pose sequences, and the two losses promote the results on fixed pose sequences.

6.5 Limitations

Although EvHandPose shows promising hand pose results even in several challenging scenarios, we find that there are still several cases in which our method fails to predict correct hand poses (shown in Figure 13). Typical cases showing large hand pose errors can be summarized as follows:

- **Motion ambiguity:** Although motion information and recurrent model are adopted to alleviate the motion ambiguity issue, it is not completely removed. It is still challenging to predict hand pose from event streams if a hand is kept stationary for a long time span;
- **New pose:** We observe that MPJPE of our method is $5 \sim 15$ mm smaller in the fixed poses than in the random poses. One possible reason is that the distribution of random poses has greater diversity, leading to a slightly performance drop in random pose sequences. This effect can be reduced by including more data with diverse hand poses;
- **Flash scenes:** Due to some inherent limitations from the DAVIS346 camera we use, a large amount of events will erupt in a short time for the scene with broad dynamic range. This phenomena causes too few effective event observations in a short period of time, which has little useful information for pose estimation. This might be improved by proposing effective temporal filter for hand pose in the future.

7 CONCLUSION

We propose a novel neural network for event-based monocular 3D hand pose estimation on sparse-labeled event streams. In order to deal with the asynchronous data format and motion ambiguity issue,

we adopt edge and hand flow representations to utilize the spatial-temporal information of event streams effectively. To tackle the sparse annotation challenge, we design contrast maximization and edge constraints in a self-supervised framework. And we construct the first large-scale real-world dataset for event-based hand pose estimation to address the domain gap between the synthetic and real data. Experiments on our dataset demonstrate that our method outperforms the recent event-based hand pose method [9] in all cases of EvRealHands testing dataset and RGB-based method [16] in challenging scenarios. Although our model has not been trained on fast motion sequences, it can achieve stable hand pose estimation at 120 fps. Our dataset and method provides a new benchmark and baseline of robust event-based 3D hand pose estimation, and they might inspire related researches in the future. We also hope to improve EvRealHands by capturing hands in outdoor scenes or using more advanced event cameras (such as [51] and [52]) with higher resolution and less noise.

ACKNOWLEDGMENTS

The authors would like to thank Yiran Zhang, Qida Hao and Bingxuan Wang for their great help to collect and annotate EvRealHands.

REFERENCES

- [1] V. Lepetit, “Recent advances in 3d object and hand pose estimation,” *arXiv preprint arXiv:2006.05927*, 2020.
- [2] P. Lichtsteiner, C. Posch, and T. Delbrück, “A 128×128 120 dB 15μ s latency asynchronous temporal contrast vision sensor,” *IEEE J. Solid State Circuits*, pp. 566–576, 2008.
- [3] A. Mitrokhin, C. Fermüller, C. Parameshwara, and Y. Aloimonos, “Event-based moving object detection and tracking,” in *2018 IEEE/RSJ International Conference on Intelligent Robots and Systems (IROS)*, 2018.
- [4] D. Gehrig, H. Rebecq, G. Gallego, and D. Scaramuzza, “Asynchronous, photometric feature tracking using events and frames,” in *Proc. of European Conference on Computer Vision (ECCV)*, 2018.
- [5] H. Rebecq, G. Gallego, E. Mueggler, and D. Scaramuzza, “EMVS: Event-based multi-view stereo—3D reconstruction with an event camera in real-time,” *International Journal of Computer Vision (IJCV)*, vol. 126, no. 12, pp. 1394–1414, 2018.
- [6] J. Hagenaaars, F. Paredes-Vallés, and G. De Croon, “Self-supervised learning of event-based optical flow with spiking neural networks,” *Advances in Neural Information Processing Systems (NeurIPS)*, 2021.
- [7] H. Rebecq, T. Horstschäfer, G. Gallego, and D. Scaramuzza, “Evo: A geometric approach to event-based 6-Dof parallel tracking and mapping in real time,” *IEEE Robotics and Automation Letters (IRAL)*, 2016.
- [8] Y. Zhou, G. Gallego, and S. Shen, “Event-based stereo visual odometry,” *IEEE Transactions on Robotics (TRO)*, vol. 37, no. 5, pp. 1433–1450, 2021.
- [9] V. Rudnev, V. Golyanik, J. Wang, H.-P. Seidel, F. Mueller, M. Elgharib, and C. Theobalt, “EventHands: Real-time neural 3D hand pose estimation from an event stream,” in *Proc. of International Conference on Computer Vision (ICCV)*, 2021.

- [10] H. Rebecq, R. Ranftl, V. Koltun, and D. Scaramuzza, “High speed and high dynamic range video with an event camera,” *IEEE Transactions on Pattern Analysis and Machine Intelligence (PAMI)*, vol. 43, no. 6, pp. 1964–1980, 2019.
- [11] M. Mostafavi, L. Wang, and K.-J. Yoon, “Learning to reconstruct HDR images from events, with applications to depth and flow prediction,” *International Journal of Computer Vision (IJCV)*, vol. 129, no. 4, pp. 900–920, 2021.
- [12] C. Zimmermann and T. Brox, “Learning to estimate 3D hand pose from single RGB images,” in *Proc. of International Conference on Computer Vision (ICCV)*, 2017.
- [13] U. Iqbal, P. Molchanov, T. B. J. Gall, and J. Kautz, “Hand pose estimation via latent 2.5 D heatmap regression,” in *Proc. of European Conference on Computer Vision (ECCV)*, 2018.
- [14] L. Ge, Z. Ren, Y. Li, Z. Xue, Y. Wang, J. Cai, and J. Yuan, “3D hand shape and pose estimation from a single RGB image,” in *Proc. of Conference on Computer Vision and Pattern Recognition (CVPR)*, 2019.
- [15] X. Zhang, Q. Li, H. Mo, W. Zhang, and W. Zheng, “End-to-end hand mesh recovery from a monocular RGB image,” in *Proc. of International Conference on Computer Vision (ICCV)*, 2019.
- [16] X. Chen, Y. Liu, Y. Dong, X. Zhang, C. Ma, Y. Xiong, Y. Zhang, and X. Guo, “MobRecon: Mobile-friendly hand mesh reconstruction from monocular image,” *Proc. of Conference on Computer Vision and Pattern Recognition (CVPR)*, 2022.
- [17] I. Oikonomidis, M. I. Lourakis, and A. A. Argyros, “Evolutionary quasi-random search for hand articulations tracking,” in *Proc. of Conference on Computer Vision and Pattern Recognition (CVPR)*, 2014.
- [18] D. Tzionas, L. Ballan, A. Srikantha, P. Aponte, M. Pollefeys, and J. Gall, “Capturing hands in action using discriminative salient points and physics simulation,” *International Journal of Computer Vision (IJCV)*, vol. 118, no. 2, pp. 172–193, 2016.
- [19] I. Oikonomidis, N. Kyriazis, and A. A. Argyros, “Tracking the articulated motion of two strongly interacting hands,” in *Proc. of Conference on Computer Vision and Pattern Recognition (CVPR)*, 2012.
- [20] L. Ballan, A. Taneja, J. Gall, L. V. Gool, and M. Pollefeys, “Motion capture of hands in action using discriminative salient points,” in *Proc. of European Conference on Computer Vision (ECCV)*, 2012.
- [21] N. Kyriazis and A. Argyros, “Scalable 3D tracking of multiple interacting objects,” in *Proc. of Conference on Computer Vision and Pattern Recognition (CVPR)*, 2014.
- [22] J. Romero, D. Tzionas, and M. J. Black, “Embodied Hands: Modeling and capturing hands and bodies together,” *ACM Transactions on Graphics (Proc. of ACM SIGGRAPH)*, vol. 36, no. 6, 2017.
- [23] Y. Cai, L. Ge, J. Cai, and J. Yuan, “Weakly-supervised 3D hand pose estimation from monocular RGB images,” in *Proc. of European Conference on Computer Vision (ECCV)*, 2018.
- [24] A. Spurr, U. Iqbal, P. Molchanov, O. Hilliges, and J. Kautz, “Weakly supervised 3D hand pose estimation via biomechanical constraints,” in *Proc. of European Conference on Computer Vision (ECCV)*, 2020.
- [25] X. Deng, Y. Zhu, Y. Zhang, Z. Cui, P. Tan, W. Qu, C. Ma, and H. Wang, “Weakly supervised learning for single depth-based hand shape recovery,” *IEEE Transactions on Image Processing (TIP)*, vol. 30, pp. 532–545, 2020.
- [26] D. Kulon, R. A. Guler, I. Kokkinos, M. M. Bronstein, and S. Zafeiriou, “Weakly-supervised mesh-convolutional hand reconstruction in the wild,” in *Proc. of Conference on Computer Vision and Pattern Recognition (CVPR)*, 2020.
- [27] Y. Chen, Z. Tu, D. Kang, L. Bao, Y. Zhang, X. Zhe, R. Chen, and J. Yuan, “Model-based 3D hand reconstruction via self-supervised learning,” in *Proc. of Conference on Computer Vision and Pattern Recognition (CVPR)*, 2021.
- [28] C. Wan, T. Probst, L. V. Gool, and A. Yao, “Self-supervised 3D hand pose estimation through training by fitting,” in *Proc. of Conference on Computer Vision and Pattern Recognition (CVPR)*, 2019.
- [29] A. Boukhayma, R. d. Bem, and P. H. Torr, “3D hand shape and pose from images in the wild,” in *Proc. of Conference on Computer Vision and Pattern Recognition (CVPR)*, 2019.
- [30] N. Neverova, J. Thewlis, R. A. Guler, I. Kokkinos, and A. Vedaldi, “Slim densepose: Thrifty learning from sparse annotations and motion cues,” in *Proc. of Conference on Computer Vision and Pattern Recognition (CVPR)*, 2019.
- [31] Y. Hasson, B. Tekin, F. Bogo, I. Laptev, M. Pollefeys, and C. Schmid, “Leveraging photometric consistency over time for sparsely supervised hand-object reconstruction,” in *Proc. of Conference on Computer Vision and Pattern Recognition (CVPR)*, 2020.
- [32] A. Z. Zhu, L. Yuan, K. Chaney, and K. Daniilidis, “EV-FlowNet: Self-supervised optical flow estimation for event-based cameras,” 2018.
- [33] —, “Unsupervised event-based learning of optical flow, depth, and egomotion,” in *Proc. of Conference on Computer Vision and Pattern Recognition (CVPR)*, 2019.
- [34] L. Xu, W. Xu, V. Golyanik, M. Habermann, L. Fang, and C. Theobalt, “EventCap: Monocular 3D capture of high-speed human motions using an event camera,” in *Proc. of Conference on Computer Vision and Pattern Recognition (CVPR)*, 2020.
- [35] S. Zou, C. Guo, X. Zuo, S. Wang, P. Wang, X. Hu, S. Chen, M. Gong, and L. Cheng, “EventHPE: Event-based 3D human pose and shape estimation,” in *Proc. of International Conference on Computer Vision (ICCV)*, 2021.
- [36] J. Nehvi, V. Golyanik, F. Mueller, H.-P. Seidel, M. Elgharib, and C. Theobalt, “Differentiable event stream simulator for non-rigid 3D tracking,” in *Proc. of Conference on Computer Vision and Pattern Recognition (CVPR)*, 2021.
- [37] J. P. Lewis, M. Corder, and N. Fong, “Pose space deformation: a unified approach to shape interpolation and skeleton-driven deformation,” in *ACM Transactions on Graphics (Proc. of ACM SIGGRAPH)*, 2000, pp. 165–172.
- [38] X. Shi, Z. Chen, H. Wang, D.-Y. Yeung, W.-K. Wong, and W.-c. Woo, “Convolutional LSTM network: A machine learning approach for precipitation nowcasting,” *Advances in Neural Information Processing Systems (NeurIPS)*, vol. 28, 2015.
- [39] G. Gallego, H. Rebecq, and D. Scaramuzza, “A unifying contrast maximization framework for event cameras, with applications to motion, depth, and optical flow estimation,” in *Proc. of Conference on Computer Vision and Pattern Recognition (CVPR)*, 2018.
- [40] G. Gallego, M. Gehrig, and D. Scaramuzza, “Focus is all you need: Loss functions for event-based vision,” in *Proc. of Conference on Computer Vision and Pattern Recognition (CVPR)*, 2019.
- [41] T. Simon, H. Joo, I. Matthews, and Y. Sheikh, “Hand keypoint detection in single images using multiview bootstrapping,” in *Proc. of Conference on Computer Vision and Pattern Recognition (CVPR)*, 2017.
- [42] S. Han, B. Liu, R. Cabezas, C. D. Twigg, P. Zhang, J. Petkau, T.-H. Yu, C.-J. Tai, M. Akbay, Z. Wang *et al.*, “MEgATrack: monochrome egocentric articulated hand-tracking for virtual reality,” *ACM Transactions on Graphics (Proc. of ACM SIGGRAPH)*, vol. 39, no. 4, pp. 87–1, 2020.
- [43] J. Heikkilä and O. Silvén, “A four-step camera calibration procedure with implicit image correction,” in *Proc. of Conference on Computer Vision and Pattern Recognition (CVPR)*, 1997.
- [44] Q. De Smedt, H. Wannous, J.-P. Vandeborre, J. Guerry, B. L. Saux, and D. Filliat, “3D hand gesture recognition using a depth and skeletal dataset: Shrec’17 track,” in *Proceedings of the Workshop on 3D Object Retrieval*, 2017.
- [45] G. Moon, S.-I. Yu, H. Wen, T. Shiratori, and K. M. Lee, “Interhand2.6M: A dataset and baseline for 3D interacting hand pose estimation from a single RGB image,” in *Proc. of European Conference on Computer Vision (ECCV)*, 2020.
- [46] C. Zimmermann, D. Ceylan, J. Yang, B. Russell, M. Argus, and T. Brox, “Freihand: A dataset for markerless capture of hand pose and shape from single RGB images,” in *Proc. of International Conference on Computer Vision (ICCV)*, 2019.
- [47] F. Zhang, V. Bazarevsky, A. Vakunov, A. Tkachenka, G. Sung, C.-L. Chang, and M. Grundmann, “Mediapipe hands: On-device real-time hand tracking,” *arXiv preprint arXiv:2006.10214*, 2020.
- [48] K. He, X. Zhang, S. Ren, and J. Sun, “Deep residual learning for image recognition,” in *Proc. of Conference on Computer Vision and Pattern Recognition (CVPR)*, 2016.
- [49] D. P. Kingma and J. Ba, “Adam: A method for stochastic optimization,” in *International Conference on Learning Representations (ICLR)*, 2015.
- [50] J. S. Supancic III, G. Rogez, Y. Yang, J. Shotton, and D. Ramanan, “Depth-based hand pose estimation: methods, data, and challenges,” *Proc. of International Conference on Computer Vision (ICCV)*, 2015.
- [51] S. Chen and M. Guo, “Live demonstration: CeleX-V: A 1M pixel multi-mode event-based sensor,” in *Proc. of Conference on Computer Vision and Pattern Recognition (CVPR) Workshops*, 2019, pp. 1682–1683.
- [52] T. Finateu, A. Niwa, D. Matolin, K. Tsuchimoto, A. Mascheroni, E. Reynaud, P. Mostafalu, F. T. Brady, L. Chotard, F. LeGoff, H. Takahashi, H. Wakabayashi, Y. Oike, and C. Posch, “A 1280×720 back-illuminated stacked temporal contrast event-based vision sensor with 4.86μm pixels, 1.066GEPS readout, programmable event-rate controller and compressive data-formatting pipeline,” in *IEEE International Solid-State Circuits Conference*, 2020, pp. 112–114.



Jianping Jiang received his B.Eng. degree from Tsinghua University, in 2020. He is currently a master graduate student in the School of Computer Science, Peking University. His research interests span event-based vision, 3D reconstruction and localization.



Jiahe Li received his B.S. degree in School of Artificial Intelligence, Beijing Normal University. He is currently a master student at the Institute of Software, Chinese Academy. His research interests include computer vision, 3D reconstruction, human motion tracking and synthesis.



Baowen Zhang received his B.Eng. degree from Southeast University, in 2020. He is currently a master graduate student at the Institute of Software, Chinese Academy of Sciences. His main research interest is computer vision.



Xiaoming Deng is currently a Professor with the Institute of Software, Chinese Academy of Sciences (CAS). He received the BS and MS degrees from Wuhan University, and the PhD degree from the Institute of Automation, CAS. He has been a Research Fellow at the National University of Singapore, and a Postdoctoral Fellow at the Institute of Computing Technology, CAS, respectively. His main research topics are in computer vision, and specifically related to 3D reconstruction, human motion tracking and synthesis, and natural user interfaces.



Boxin Shi received the BE degree from the Beijing University of Posts and Telecommunications, the ME degree from Peking University, and the PhD degree from the University of Tokyo, in 2007, 2010, and 2013. He is currently a Boya Young Fellow Assistant Professor and Research Professor at Peking University, where he leads the Camera Intelligence Lab. Before joining PKU, he did postdoctoral research with MIT Media Lab, Singapore University of Technology and Design, Nanyang Technological University from 2013 to

2016, and worked as a researcher in the National Institute of Advanced Industrial Science and Technology from 2016 to 2017. His papers were awarded as Best Paper Runner-Up at International Conference on Computational Photography 2015 and selected as Best Papers from ICCV 2015 for IJCV Special Issue. He has served as an editorial board member of IJCV and an area chair of CVPR/ICCV. He is a senior member of IEEE.